THE TAIWAN IONOSPHERIC MODEL (TWIM) AND ITS APPLICATIONS ON RADIO WAVE PROPAGATION AND IONOSPHERIC GPS L1 PSEUDORANGE CORRECTION

L.-C. Tsai[a, b], G. H. Chen[c], M. H. Tian[d], and Ernest P. Macalalad[b]

[a] Center for Space and Remote Sensing Research, National Central University (NCU), Chung-Li, Taiwan; lctsai@csrsr.ncu.edu.tw

[b] Graduate Institute of Space Science, NCU, Chung-Li, Taiwan

[c] Multimedia and Game Science Department, Taipei College of Maritime Technology (TCMT), Taipei, Taiwan

[d] Department of Marine Leisure and Tourism, TCMT, Taipei, Taiwan

KEY WORDS: Ionospheric electron density model, GPS radio occultation, GPS positioning

ABSTRACT

A three-dimensional ionospheric electron density (N_e) model has been named the TaiWan Ionospheric Model (TWIM) and constructed from monthly-weighted and hourly vertical N_e profiles retrieved from FormoSat3/COSMIC GPS radio occultation (RO) measurements. The TWIM exhibits vertically-fitted α-Chapman-type layers, with distinct F2, F1, E, and D layers, and surface spherical harmonics approaches for the fitted layer parameters including peak density, peak density height, and scale height. These results are useful in investigation of near-Earth space and large-scale N_e distribution. This way the continuity of N_e and its derivatives is also maintained for practical schemes for providing reliable radio propagation predictions. We also present a numerical and step by step ray-tracing method on the TWIM. With the Earth's magnetic field and horizontal N_e gradient effects included, efficient methods for calculating ray parameters such as phase path and group path are presented. The methodology has been successfully applied to a practical high-frequency transmitter for oblique incidence ray tracing and further evaluated by comparing synthetic vertical ionograms generated by the method with experimental ionosonde observations. Furthermore, the ray-tracing methodology also has potential applicability to ionospheric correction as applied to single frequency GPS receivers. In this paper, ionospheric delay correction for single-frequency GPS pseudoranges using the TWIM is presented. Its performance with respect with the ionospheric correction using other ionospheric model and the dual-frequency GPS receiver will also be presented.

1. SPACED-BASED GPS RADIO OCCULTATION OBSERVATIONS AND THE TAIWAN IONOSPHERIC MODEL (TWIM)

The TWIM is constructed from the Taiwan FormoSat3 / Constellation Observing System for Meteorology, Ionosphere and Climate (FS3/COSMIC) data mostly. The FS3/COSMIC program includes six spacecraft (FM1 to FM6) located at a nearly circular orbit of ~800 km altitude, ~70° inclination angle, and 60° separation to receive GPS signals. The Global Positioning System (GPS) radio occultation (RO) technique has been used to receive multi-channel GPS carrier phase signals at low Earth orbiting (LEO) satellites performing active limb sounding of the Earth's atmosphere and ionosphere. Generally FS3/COSMIC can obtain over 2500 RO measurements per day, providing data for the atmosphere and ionosphere including areas over the oceans, the southern hemisphere, where few ground-based stations are located. For further details about the FS3/COSMIC program, see [*Rocken et al.*, 2000; *Hajj et al.*, 2000]. Each GPS RO observation consists of a set of limb-viewing links with tangent points ranging from the LEO satellite orbit altitude to the Earth's surface. The path TEC values are obtained from differential GPS phase measurements using both the L1 and L2 radio signals. The N_e values can be retrieved from the calibrated or compensated TEC values [*Schreiner et al.*, 1999; *Tsai et al.*, 2009a] using the Abel integral transform given by *Tricomi* [1985] defined as:

$$N_e(r_t) = -\frac{1}{\pi}\int_{r_t}^{r_{LEO}} \frac{dTEC(r)/dr}{\sqrt{r^2 - r_t^2}}\, dr\,. \qquad (1)$$

The N_e value at a tangent point's radial distance r_t can be computed in a recursive way starting from the outmost ray at r_{LEO} and its N_e profile can then be obtained to the base of the ionosphere.

The terrestrial ionosphere at all latitudes has a tendency to separate into layers at different altitude regions. Specifically, the N_e profiles exhibit layered structures, with distinct F2, F1, E, and D layers, despite the fact that different physical processes dominate in different latitudinal region. In the TWIM each layer is generally characterized by a Chapman-type function described by the parameters of peak N_e (N_{emax}), peak density height (h_m), and scale height (H), and the layer parameters can be obtained with least-squares error fitting of the observed profile to the Chapman functions.

$$N_e(\theta,\lambda,h) = \sum_{i=1}^{4} N_{e\max}^{i}(\theta,\lambda)\cdot e^{\frac{1}{2}\left(1-\frac{h-h_m^i(\theta,\lambda)}{H^i(\theta,\lambda)}-e^{-\frac{h-h_m^i(\theta,\lambda)}{H^i(\theta,\lambda)}}\right)} \qquad (2)$$

where each i means a physical layer of F2, F1, E, or D layer. A Chapman-type layer is predicted by a simplified aeronomic theory, assuming photoionization in a one-species neutral gas, and neglecting transport processes. All of the layers are usually present during the daytime. The F1 and D layers decay at night and could be hidden within the other layers, but the F1- and D-layer parameters are still derivable throughout all times by least-squares

error fitting. In the TWIM a two-dimensional (latitude and longitude) numerical map to fit derived layer peak N_e, peak density height, or scale height values can be represented by a function $\Gamma(\theta, \lambda)$ and constructed by spherical harmonic analysis of the Laplace's partial differential equation. The resulting real functions of θ (latitude) and λ (longitude or the local time angle) are combinations of the surface spherical harmonics [*Davis*, 1989] defined by

$$\Gamma(\theta,\lambda) = \sum_{m=0}^{3}\sum_{n=0}^{q_m}\left[A_{nm}\, U_{nm}(\theta,\lambda) + B_{nm}\, V_{nm}(\theta,\lambda)\right], \text{where}$$

$$U_{nm}(\theta,\lambda) = \sqrt{\frac{2n+1}{2\pi}\frac{(n-m)!}{(n+m)!}}\, P_n^m(\cos\theta)\cos m\lambda \text{ , and}$$

$$V_{nm}(\theta,\lambda) = \sqrt{\frac{2n+1}{2\pi}\frac{(n-m)!}{(n+m)!}}\, P_n^m(\cos\theta)\sin m\lambda \qquad (3)$$

$$(n = 0, 1, 2, \cdots q_m \text{ ; } m = 0, 1, 2, \textit{or } 3),$$

and $P_n^m( )$ is the familiar associated Legendre polynomial of the first kind of degree n and order m. After the optimization analyses of noise separation we determined the cutoffs to be an order of 3 and a degree of 20 for each order. For details concerning the performance and evaluation of the TWIM, the interested readers are referred to *Tsai et al.* [2009b]. The three spherical components of N_e gradients are given by

$$\frac{\partial N_e}{\partial h} = \sum_{i=1}^{4} N_{e\max}^{i} \cdot e^{\frac{1}{2}\left(1-x_i-e^{-x_i}\right)} \cdot \left(-\frac{1}{2}+\frac{1}{2}e^{-x_i}\right)\cdot H^i \text{ ,}$$

$$\frac{1}{r}\frac{\partial N_e}{\partial \theta} = \frac{1}{r}\cdot\left[\begin{array}{l}\displaystyle\sum_{i=1}^{4} e^{\frac{1}{2}\left(1-x_i-e^{-x_i}\right)}\cdot\frac{\partial N_{e\max}^{i}}{\partial\theta} + \\ \displaystyle\sum_{i=1}^{4} N_{e\max}^{i}\cdot e^{\frac{1}{2}\left(1-x_i-e^{-x_i}\right)}\cdot\left(-\frac{1}{2}+\frac{1}{2}e^{-x_i}\right)\cdot\left(-\frac{1}{H^i}\frac{\partial h_m^i}{\partial\theta}-\frac{h-h_m^i}{H^{i2}}\frac{\partial H^i}{\partial\theta}\right)\end{array}\right]$$

$$\frac{1}{r\sin\theta}\frac{\partial N_e}{\partial \phi} = \frac{1}{r\sin\theta}\cdot\left[\begin{array}{l}\displaystyle\sum_{i=1}^{4} e^{\frac{1}{2}\left(1-x_i-e^{-x_i}\right)}\cdot\frac{\partial N_{e\max}^{i}}{\partial\phi} + \\ \displaystyle\sum_{i=1}^{4} N_{e\max}^{i}\cdot e^{\frac{1}{2}\left(1-x_i-e^{-x_i}\right)}\cdot\left(-\frac{1}{2}+\frac{1}{2}e^{-x_i}\right)\cdot\left(-\frac{1}{H^i}\frac{\partial h_m^i}{\partial\phi}-\frac{h-h_m^i}{H^{i2}}\frac{\partial H^i}{\partial\phi}\right)\end{array}\right], \qquad (4)$$

where $x_i = (h-h_m^i)/H^i$, and i means one of the F2, F1, E, and D physical layers. The phenomenological ionospheric model thus provides temporal and synoptic variations in three-dimensional (latitude, longitude, and altitude) N_e and maintains the continuity in the first and second N_e derivatives for providing reliable radio propagation predictions and electrostatic field determinations.

2. RAY-TRACING SCHEME AND RAY-TRACING RESULTS

Wave propagation can be described by a complicated solution to the Maxwell's equations but, in the case of HF radio waves propagating in a non-absorbing ionosphere, a geometric optics approach is adequate for ray tracing. Upon incident on a TWIM modeled ionosphere and at each step of the ray tracing, the N_e values and N_e gradients at the intersected positions can be determined with the TWIM at specified universal time (UT). Meanwhile, the Earth's magnetic field is assumed as the model with an Earth centered dipole and to fall as $1/r^3$. Therefore, this study deals with the propagation of plane waves in a slowly varying anisotropic ionosphere. A full three dimensional ray tracing is simulated upon independent vectors of initial ray direction, *Ne* gradient, and magnetic field. The start point for this ray-tracing development is the Fermat's principle of least stationary time, i.e. a ray between two points is the path such that the optical path length has a stationary value. In an anisotropic medium this principle can be expressed in the form

$$\delta \int n_r \, ds = \delta \int \mu \cos \alpha \; d s = 0, \tag{5}$$

where n_r is the ray refractive index, μ is the phase refractive index of non-absorbing ionosphere, α is the angle between the wave vector and the ray direction, and *ds* is an element of arc length along the ray path. Next, applying the Euler-Lagrange Equations, we derive a generalized differential form of Snell's Law [*Kelso*, 1964] and the corresponding wave normal number *u* and its unit vector $\hat{u}$ can be obtained as follows:

$$\frac{d}{dP}(\mu \, \hat{u}) = \frac{1}{u} \, \overline{\nabla} \mu \, , \tag{6}$$

where *P* is the phase path. Since we are dealing with an anisotropic ionosphere with the Earth's magnetic field but without losses due to collisions, the refractive index μ is given by the Appleton-Lassen or the Appleton-Hartree formula [*Appleton*, 1932; *Hartree*, 1931], which represents the two magnetoionic modes of ordinary and extraordinary characteristic waves. This paper will include families of rays and contributions associated with both modes. Meanwhile, we assume that the refractive index gradient coincides with the N_e gradient. In the presence of a non-uniform magnetic field the two gradients should differ, but the effect is always less than 10^{-4} radian at ionospheric heights and can be neglected, although it would have to be included for ray tracing in the exosphere. The ray is situated in the plane defined by the wave normal and the Earth's magnetic field [*Bremmer*, 1949] and has the angle α from the wave normal to the ray direction as

$$\tan \alpha = \pm \frac{\left(\mu^2 - 1\right) Y \sin \Theta \cos \Theta}{\left[Y^2 \sin^4 \Theta + 4 \left(1 - X\right)^2 \cos^2 \Theta \right]^{0.5}} \, . \tag{7}$$

The + and – signs refer to the ordinary and extraordinary waves respectively, $X = f_N{}^2 / f^2$ where f_N is the plasma frequency and f is the radio frequency, $Y = f_H / f$ where f_H is the gyrofrequency, and Θ is the angle between $\hat{u}$ and the Earth's magnetic field.

The ray-tracing scheme presented here calculates integration steps of equal length in an independent variable of elapsed group path (or time of flight). It eases the true-path step size changes required, because, especially near the ray-tracing reflector, when the ray geometry is changing more slowly at an equal length of group path than true path. The computation proceeds step by step from a given set of radio frequency, universal time, time of flight interval, and initial values of transmitter or receiver position, launch or arriving azimuth and elevation angles for forward or backward ray tracing, respectively. Once the launch or arriving azimuth and elevation angles of a ray have been specified, ray tracing begins from a known transmitter or receiver, and the wave vector and ray direction of the beginning path step can be determined. For convenience, assume that the ray is traveling straight along each short step distance within a constant time of flight and then enters a new path step. Through a TWIM modeled ionosphere the general Snell's law applies and a new wave vector can be determined from Eq. (6), and then a new ray direction is obtained from Eq. (7) and from one path step to the next. After each step along the path is traced, the new aiming ray position is computed by adding the distance vector to the old aiming position. The step distance is determined by the product of time step and the ray velocity (or packet velocity), the magnitude of which is defined by

$$v_r = \frac{c}{\mu' \cos\alpha}, \qquad (8)$$

where c is the light speed in free space, and μ' is the real group refractive index and can be determined by the equations published by *Shinn and Whale* [1952]. Thus the ray could be up through the ionosphere or reflected and back down to the ground. We note that it is clearly more efficient for the time of flight interval to be large, however, one needs to limit the truncation error. A value of 10^{-5} sec has been used in this study. Figures 1a, 1b, and 1c show ray-tracing paths in top-viewing and latitudinal and longitudinal side-viewing for a central ray and four side rays into a TWIM modeled ionosphere and considering the horizontal N_e gradients from the TWIM and the Earth's magnetic field. The figures also show background imaging colors representing the modeled critical plasma frequencies, i.e. *foF2*, in Figure 1a and modeled plasma frequencies in Figures 1b and 1c of the TWIM at 4:00 UT on Dec. 15, 2007. The transmitter was placed at Chung-Li (24.97°N, 121.19°E), Taiwan. The central ray are shown in white and has an azimuthal angle of 300° and an elevation angle of 15°, and four side rays in red and blue are related a half-power angle of 10° to the central rays. It is noted that the corresponding ionospheric N_e is related to plasma frequency (f_N) in accordance with the conversion formula f_N^2 (MHz) = 80.6 N_e (cm^{-3}).

3. CONCLUDING REMARKS

An algorithm has been developed that can trace radio rays on a numerical ionospheric model of TWIM constructed from the F3/COSMIC data. The TWIM is intended to model

large-scale and statistical N_e variations. It provides three-dimensional N_e distributions with vertically-fitted Chapman layers that have distinct F2, F1, E, and D layers, for which surface spherical harmonics approaches were used to represent the Chapman-layer parameters. The continuity of N_e and its derivatives is maintained in this model which allows practical schemes for providing reliable radio propagation prediction and electrostatic field determination. It has been shown that the stepped ray tracing described here allows for the inclusion of horizontal N_e gradients and the three dimensional Earth's magnetic field along the ray. There are several areas in which the current ray-tracing algorithm could be improved. The most important is to improve the accuracy of N_e specification. The TWIM has been developed to model large-scale and statistical N_e variations, and thus increasing its temporal and spatial resolutions could provide better N_e specification which in turn will improve ray-tracing accuracy. Next, the centered-dipole field which is used as approximation to the geomagnetic field is sufficient for many purposes, but, for very accurate ray-tracing, the magnetic field can be replaced by a more complete representation on spatial resolution. Future works should also include the effect of electron collision and wave amplitudes estimation.

Acknowledgements. This work has been supported by Projects 98-NSPO(B)-IC- FA07-01(I), NSC98-2111-M-008-013-MY3, and NSC97-2111-M008-008-024-MY2.

REFERENCES

Appleton, E. V. (1932), Wireless studies of the ionosphere, *J. Instn Elect. Engrs.*, 71, 642-650.

Bremmer, H. (1949), *Terrestrial radio waves*, Elsevier Publishing Company, Inc., New York.

Davis, Harry F. (1989), *Fourier series and orthogonal functions*, Dover Publications, Inc., New York.

Hajj, G. A., L. C. Lee, X. Pi, L. J. Romans, W. S. Schreiner, P. R. Straus, and C. Wang (2000), COSMIC GPS ionospheric sensing and space weather, *Terrestial, Atmospheric and Oceanic Sciences*, 11(1), 235-272.

Hartree, D. R. (1931), The propagation of electromagnetic waves in a refracting medium in a magnetic field, *Proc. Camb. Phil. Soc.*, 27, 143-162.

Kelso, John M. (1964), *Radio ray propagation in the ionosphere*, McGraw-Hill Book Company, New York.

Rocken, Christian, Y.-H. Kuo, W. Schreiner, D. Hunt, S. Sokolovskiy, and C. McCormick (2000), COSMIC system description, *Terrestial, Atmospheric and* Oceanic Sciences, 11(1), 21-52.

Schreiner, W. S., S. V. Sokolovskiy, C. Rocken, and D. C. Hunt (1999), Analysis and validation of GPS/MET radio occultation data in the ionosphere, *Radio Sci., 34(4)*, 949-966.

Shinn, D. H. and Whale, H. A. (1952), Group velocities and group heights from the

magnetoionic theory, *J. Atmos. Terr. Phys. 2*, 85-105.

Tricomi, F. G. (1985), *Integral Equations*, 238 pages, Dover, Mineola, New York.

Tsai, L.-C., C. H. Liu, and T. Y. Hsiao (2009a), Profiling of ionospheric electron density based on the FormoSat-3/COSMIC data: results from the intense observation period experiment, *Terrestial, Atmospheric and Oceanic Sciences*, 20 *(1)*, 181-191, doi: 10.3319/TAO.2007.12.19.01 (F3C).

Tsai, L.-C., C. H. Liu, T. Y. Hsiao, and J. Y. Huang (2009b), A near real-time phenomenological model of ionospheric electron density based on GPS radio occultation data, *Radio Sci., 44*, doi:10.1029/2009RS004154.

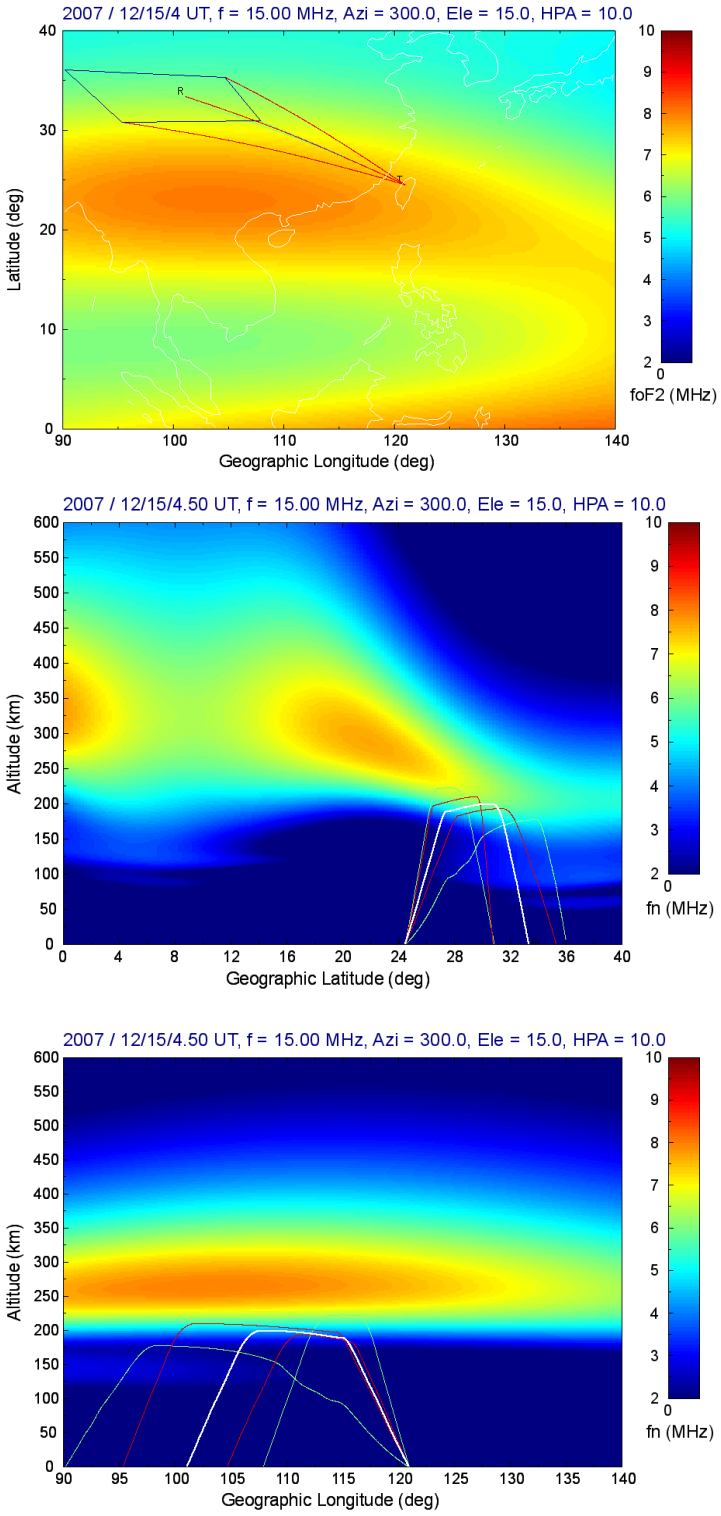

Figure 1. Example ray-tracing paths are shown in top-viewing as the top figure (Figure 1a) and latitudinal and longitudinal side-viewing as the central and bottom figures (Figures 1b and 1c), respectively. Ray-tracing paths include a central ray colored in white and four side rays colored in red and blue into a TWIM modeled ionosphere and considering the horizontal N_e gradients from the TWIM and the Earth's magnetic field. The background imaging colors represent the modeled critical plasma frequencies, i.e. *foF2*, in Figure 1a and modeled plasma frequencies in Figures 1b and 1c of the TWIM at 4:00 UT on Dec. 15, 2007.